Mon. Not. R. Astron. Soc. **000**, 1–?? (1994) Printed 5 February 2008 (MN LATEX style file v1.4)

On the magnetic acceleration and collimation of astrophysical outflows

S. Bogovalov[1⋆] and K. Tsinganos[2,3⋆]

[1] *Astrophysics Institute of Moscow State Engineering Physics Institute, Moscow, 115409, Russia*
[2] *Department of Physics, University of Crete, GR-710 03 Heraklion, Crete, GREECE*
[3] *Foundation for Research and Technology Hellas (FORTH), GR-711 10 Heraklion, Crete, GREECE*

arXiv:astro-ph/9901081v1 8 Jan 1999

Accepted 1998 November 29. Received September 11, 1998; in original form 1998 April 29

ABSTRACT

The axisymmetric 3-D MHD outflow of cold plasma from a magnetized and rotating astrophysical object is numerically simulated with the purpose of investigating the outflow's magnetocentrifugal acceleration and eventual collimation. Gravity and thermal pressure are neglected while a split-monopole is used to describe the initial magnetic field configuration. It is found that the stationary final state depends critically on a single parameter α expressing the ratio of the corotating speed at the Alfvén distance to the initial flow speed along the initial monopole-like magnetic fieldlines. Several angular velocity laws have been used for relativistic and nonrelativistic outflows. The acceleration of the flow is most effective at the equatorial plane and the terminal flow speed depends linearly on α. Significant flow collimation is found in nonrelativistic efficient magnetic rotators corresponding to relatively large values of $\alpha \gtrsim 1$ while very weak collimation occurs in inefficient magnetic rotators with smaller values of $\alpha < 1$. Part of the flow around the rotation and magnetic axis is cylindrically collimated while the remaining part obtains radial asymptotics. The transverse radius of the jet is inversely proportional to α while the density in the jet grows linearly with α. For $\alpha \gtrsim 5$ the magnitude of the flow in the jet remains below the fast MHD wave speed everywhere. In relativistic outflows, no collimation is found in the supersonic region for parameters typical for radio pulsars. All above results verify the main conclusions of general theoretical studies on the magnetic acceleration and collimation of outflows from magnetic rotators and extend previous numerical simulations to large stellar distances.

Key words: Key-words: MHD - plasmas - stars: mass loss, atmosphere, pulsars - ISM: jets and outflows - galaxies: jets

1 INTRODUCTION

Plasma outflows from the environment of stellar or galactic objects, in the form of collimated jets is a widespread phenomenon in astrophysics. The most dramatic illustration of such highly collimated outflows may be perhaps found in relatively nearby regions of star formation; for example, in the Orion Nebula alone the Hubble Space Telescope (HST) has observed hundreds of aligned Herbig-Haro objects (O'Dell & Wen, 1994). In particular, recent HST observations show that several jets from young stars are highly collimated within 30 - 50 AU from the source star with jet widths of the order of tens of AU, although their initial opening angle is rather large, e.g., $> 60^o$, Ray et al (1996). There is also a long catalogue of jets associated with AGN and possibly supermassive black holes (Jones and Wehrle 1994, Biretta 1996). To a less extend, jets are also associated with older mass losing stars and planetary nebulae, (Livio 1997), symbiotic stars (Kafatos 1996), black hole X-ray transients (Mirabel & Rodriguez 1996), supersoft X-ray sources (Kahabka & Trumper 1996), low- and high-mass X-ray binaries and cataclysmic variables (Shahbaz et al 1997). Even for the two spectacular rings seen with the HST in SN87A, it has been proposed that they may be inscribed by two precessing jets from an object similar to SS433 on a hourglass-shaped cavity which has been created by nonuniform winds of the progenitor star (Burderi and King, 1995, Burrows et al 1995).

In the theoretical front, the morphologies of collimated outflows have been studied, to a first approximation, in the framework of ideal stationary or time-dependent magneto-

⋆ Email: bogoval@photon.mephi.ru (SB); tsingan@physics.uch.gr (KT)

© 1994 RAS

hydrodynamics (MHD). In *stationary* studies, after the pioneering 1-D (spherically symmetric) works of Parker (1963), Weber & Davis (1967) and Michel (1969), it was Suess (1972) and Nerney & Suess (1975) who first modelled the 2-D (axisymmetric) interaction of magnetic fields with rotation in stellar winds, by a linearisation of the MHD equations in inverse Rossby numbers. Although their perturbation expansion is not uniformly convergent but diverges at infinity, they found a poleward deflection of the streamlines of the solar wind caused by the toroidal magnetic field. Blandford & Payne (1982) subsequently demonstrated that astrophysical jets may be accelerated magnetocentrifugally from Keplerian accretion disks, *if* the poloidal fieldlines are inclined by an angle of 60^o, or less, to the disk midplane (but see also, Contopoulos & Lovelace (1994), Shu et al, 1994, Cao, 1997, Meier et al 1997). This study introduced the "bead on a rigid wire" picture, although these solutions are limited by the fact that they contain singularities along the system's axis and also terminate at finite heights above the disk. Sakurai (1985) extended the Weber & Davis (1969) equatorial solution to all space around the star by iterating numerically between the Bernoulli and transfield equations; thus, a polewards deflection of the poloidal fieldlines was found not only in an initially radial magnetic field geometry, but also in a split-monopole one appropriate to disk-winds, Sakurai (1987). The methodology of meridionally self-similar exact MHD solutions with a variable polytropic index was first introduced by Low & Tsinganos (1986) and Tsinganos & Low (1989) in an effort to model the *heated* axisymmetric solar wind. Heyvaerts & Norman (1989) have shown analytically that the asymptotics of a particular fieldline in non isothermal polytropic outflows is parabolic if it does not enclose a net current to infinity; and, if a fieldline exists which does enclose a net current to infinity, then, somewhere in the flow there exists a cylindrically collimated core. Later, Bogovalov (1995) showed analytically that there *always* exists a fieldline in the outflowing part of a *rotating* magnetosphere which encloses a finite total poloidal current and therefore the asymptotics of the outflow *always* contains a cylindrically collimated core. In that connection, it has been shown in Bogovalov (1992) that the poloidal fieldlines are deflected towards the polar axis for the split monopole geometry and relativistic or nonrelativistic speeds of the outflowing plasma. Sauty & Tsinganos (1994) have self-consistently determined the shape of the fieldlines from the base of the outflow to infinity for nonpolytropic cases and provided a simple *criterion* for the transition of their asymptotical shape from conical (in inefficient magnetic rotators) to cylindrical (in efficient magnetic rotators). They have also conjectured that as a young star spins down loosing angular momentum, its collimated jet-type outflow becomes gradually a conically expanding wind. Nevertheless, the degree of the collimation of the solar wind at *large* heliocentric distances remains still observationally unconfirmed, since spacecraft observations still offer ambiguous evidence on this question. Another interesting property of collimated outflows has emerged from studies of various self-similar solutions, namely that in a large portion of them cylindrical collimation is obtained only after some oscillations of decaying amplitude in the jet-width appear (Vlahakis & Tsinganos 1997). Radially self-similar models with cylindrical asymptotics for self-collimated and magnetically dominated outflows from accretion disks have been constructed in Ostriker (1997). All existing cases of self-similar, jet- or, wind-type exact MHD solutions can be unified by a systematic analytical treatment wherein the available today examples of exact solutions emerge as special cases of a general formulation while at the same time new families with various asymptotical shapes, with (or without) oscillatory behaviour emerge as a byproduct of this systematic method (Vlahakis & Tsinganos, 1998). Altogether, some general trends on the behaviour of stationary, analytic, axisymmetric MHD solutions for MHD outflows seem to be well at hand.

However, observations seem to indicate that jets may inherently be variable. Thus, time-dependent simulations may be useful for a detailed comparison with the observations. Uchida & Shibata (1985) were the first to perform time-dependent simulations and demonstrate that a vertical disk magnetic field if twisted by the rotation of the disk can launch bipolar plasma ejections through the torsional Alfvén waves it generates. However, this mechanism applies to fully episodic plasma ejections and no final stationary state is reached to be compared with stationary studies. Similar numerical simulations of episodic outflows from Keplerian disks driven by torsional Alfvén waves on an initially vertical magnetic field have been presented by Ouyed & Pudritz (1997a,b). Goodson et al (1997) have proposed a time-dependent jet launching and collimating mechanism which produces a two-component outflow: hot, well collimated jet around the rotation axis and a cool but slower disk-wind. Stationary MHD jet-type outflows have been found in the study of Romanova et al (1997), as the asymptotic state of numerical simulations wherein a small initial velocity is given in the plasma in a tapered monopole-like magnetic field. Numerical viscosity however results in nonparallel flow and magnetic fields in the poloidal plane in the limited grid space of integration. Washimi & Shibata (1993) modelled axisymmetric thermo-centrifugal winds with a *dipole* magnetic flux distribution $B_p^2(\theta) \propto (3\cos^2\theta + 1)$ on the stellar surface (and a radial field in Washimi 1990). In this case the magnetic pressure distribution varies approximately as $B_\phi^2 \propto B_p^2 \sin^2\theta$ such that it has a maximum at about $cos^{-1}2\theta_o \approx -1/3$, or, $\theta_0 \approx 55^o$. As a result, the flow and flux is directed towards the pole and the equator from the midlatitudes around θ_o. The study was performed for uniform in latitude rotation rates and up to 60 solar radii in the equatorial plane. Bogovalov (1996, 1997) modelled numerically the effects of the Lorentz force in accelerating and collimating a cold plasma with an initially monopole-type magnetic field, in a region limited also by computer time, i.e., the near zone to the central spherical object.

This paper presents an extension of the previous results to *large* distances from the star by using a new method for the continuation of the small simulation box solution to very large distances. It also examines the efficiency of magnetic rotators of various strengths in transforming rotational energy to directed kinetic energy and how a wide range of rotation rates affects the poloidal geometry of a magnetic field. In order to achieve these objectives, the rather complicated nature of the problem requires that we start by limiting the investigation to the simplest model of cold plasma flow in a uniform in latitude monopole magnetic field along which there is an outflow with velocity V_o, as the initial condition. This simplification allows us to better study and understand

the nonlinear effects of the magnetocentrifugal forces alone in shaping the final stationary configuration. At the same time, however, it does not allow us to perform a direct comparison of the obtained results with observations. Clearly this is not the goal of the present paper since for such a comparison we need to include gravity and thermal pressure in our computations. Such a study has been already performed in the context of the solar wind and it will be presented elsewhere.

The paper is organised as follows. In Secs. 2 and 3, the initial configuration used together with the method for the numerical simulation in the nearest zone is discussed. In Secs. 4 and 5 the analytical method for extending the integration to unlimited large distances outside the near zone are briefly described. In Secs. 6 and 7 we discuss the results in the near zone containing the critical surfaces and in the asymptotic regime of the collimated outflow, for a uniform rotation. In Sec. 8 a rotation law appropriate for an accretion disk is used, while in Sec. 9 we briefly discuss results of a relativistic modelling. A brief summary is finally given in the last Section 9.

2 THE MODEL OF A ROTATOR WITH A MONOPOLE-LIKE MAGNETIC FIELD AND THE OBJECTIVES OF THIS PAPER

A general analysis of the asymptotical properties of nonrelativistic or relativistic magnetized winds has been already performed, e.g., Heyvaerts and Norman (1989), Chiueh et al (1991), Bogovalov (1995). The main conclusions from such studies can be summarized as follows:

(i) At large distances from the central source the poloidal magnetic field is similar (although not exactly the same) to a split-monopole field,
(ii) there exist cylindrically collimated and radially expanding field lines, while the total electric current enclosed by any magnetic surface is nonzero,
(iii) several physical quantities accross the jet can be expressed by simple formulas, under certain conditions.

The model of an axisymmetric rotator with a monopole-like magnetic field was first used by Michel (1969) for the investigation of the cold plasma flow in the absense of gravity in a prescribed poloidal magnetic field. Later this model was used by Sakurai (1985) in an attempt to solve selfconsistently the problem of the nonrelativistic plasma outflow from a stellar object. This model may be used to the study of plasma outflow from the magnetospheres of various cosmic objects under the following conditions:

(1) We are interested in the plasma flow at *large* distances where all magnetic field lines are open. In this case, the field of any axisymmetric rotator, no matter what is the nature of the central object, becomes the field of the so-called split-monopole in the far zone. In other words, the condition that should be fulfilled is that the distance to the central source should be much larger than all the dimensions of the central source (see also Heyvaerts & Norman 1989, Bogovalov 1995). The solution for the split monopole field can be easily obtained from a monopole-like solution by a simple reversing of the magnetic field in one of the hemispheres.

(2) In considering the plasma flow at such large distances it is natural to neglect gravity. Thermal pressure however may play an important role even at large distances from the central object (Bogovalov 1995). But in this paper we are interested to isolate the effects arising purely from the magnetic field. Thus, to make our analysis as simple as possible, in this paper we neglect thermal pressure too.

(3) We are also interested to study the magnetocentrifugal acceleration of the plasma. This acceleration process can be studied with a monopole like magnetic field regarded as a first approximation to the more realistic acceleration in a dipole-like magnetic field with open field lines. Gravity and thermal pressure can be neglected in this case (Michel 1969).

The previous claims (i) - (iii) are the result of a rather general analysis. Among the main goals of the present work is to verify these general conclusions in the context of the split monopole model and assumptions (1) - (3).

3 THE PROBLEM IN THE NEAREST ZONE.

To obtain a stationary solution of the problem in the nearest zone of the star containing the critical surfaces, it is needed to solve the complete system of the time-dependent MHD equations and look for an asymptotic stationary state. In order to isolate the effects of the magnetic field in determining the shape of the streamlines, we shall neglect gravity and thermal pressure gradients, as discussed above. With these simplifications, the flow of the nonrelativistic plasma is described by the set of the familiar MHD equations,

$$\mathbf{B_p} = \frac{\nabla\psi \times \hat{\varphi}}{r}., \tag{1}$$

$$\frac{\partial\psi}{\partial t} = -V_r\frac{\partial\psi}{\partial r} - V_z\frac{\partial\psi}{\partial z}\,, \tag{2}$$

$$\frac{\partial\rho}{\partial t} = -\frac{1}{r}\frac{\partial}{\partial r}(\rho r V_r) - \frac{\partial}{\partial z}(\rho V_z)\,, \tag{3}$$

$$\frac{\partial B_\varphi}{\partial t} = \frac{\partial}{\partial z}(V_\varphi B_z - V_z B_\varphi) - \frac{\partial}{\partial r}(V_r B_\varphi - V_\varphi B_r)\,, \tag{4}$$

$$\begin{aligned}\frac{\partial V_\varphi}{\partial t} &= -\frac{V_r}{r}\frac{\partial}{\partial r}(rV_\varphi) - V_z\frac{\partial V_\varphi}{\partial z} + \\ &\frac{1}{4\pi\rho}\left(B_r\frac{\partial}{r\partial r}(rB_\varphi) + B_z\frac{\partial B_\varphi}{\partial z}\right)\,,\end{aligned} \tag{5}$$

$$\begin{aligned}\frac{\partial V_z}{\partial t} &= -V_r\frac{\partial V_z}{\partial r} - V_z\frac{\partial V_z}{\partial z} - \frac{1}{8\pi\rho r^2}\frac{\partial}{\partial z}(rB_\varphi)^2 - \\ &\frac{B_r}{4\pi\rho}\left(\frac{\partial B_r}{\partial z} - \frac{\partial B_z}{\partial r}\right)\,,\end{aligned} \tag{6}$$

$$\frac{\partial V_r}{\partial t} = -V_r\frac{\partial V_r}{\partial r} - V_z\frac{\partial V_r}{\partial z} - \frac{1}{8\pi\rho r^2}\frac{\partial}{\partial r}(rB_\varphi)^2 + \frac{V_\varphi^2}{r} + \frac{B_z}{4\pi\rho}\left(\frac{\partial B_r}{\partial z} - \frac{\partial B_z}{\partial r}\right), \quad (7)$$

where we have used cylindrical coordinates (z, r, φ), ρ is the density, $\vec{V}$ the flow field and $\vec{B}$ the magnetic field with a poloidal magnetic flux denoted by $\psi(z, r)$.

A correct solution of the problem requires a specification of the appropriate boundary conditions at some spherical boundary $R = R_o$ of the integration.
1. A constant plasma density ρ_o at $R = R_o$.
2. A constant total plasma speed V_o in the corotating frame of reference at $R = R_o$, $V_{(r,o)}^2 + V_{(z,o)}^2 + (V_{(\varphi,o)} - \Omega r_o)^2 = V_o^2$
3. A constant and uniform in latitude distribution of the magnetic flux function $\psi = \psi_o$ at $R = R_o$.
4. Finally, the continuity of the tangential component of the electric field across the stellar surface in the corotating frame gives the last condition, $(V_{(\varphi,o)} - \Omega r_o)B_{(p,o)} - V_{(p,o)}B_{(\varphi,o)} = 0$.

We shall use dimensionless variables, $Z = z/R_a$, $X = r/R_a$, $\tau = tV_0/R_a$ where R_a is the Alfvén spherical radius of an initially radial, monopole-like, nonrotating magnetic field and define the dimensionless parameter

$$\alpha = \frac{\Omega R_a}{V_0}. \quad (8)$$

This parameter α characterizes the influence of the magnetic field and rotation on the acceleration and collimation of the plasma. It is proportional to the time the plasma spends in the subAlfvenic region in each period of rotation. Note that although the governing equations (1-7) do not depend on α, the final solution does depend on α through the boundary conditions at the base of the integration $R = R_o$ (condition 4).

As we shall see, the solution in the nearest zone will relax after sufficient time to a stationary state. This stationary state will be next used as the input for specifying the boundary conditions in the super-fast magnetosonic region. In this way we shall be able to obtain a complete solution of the stationary problem, from the base up to large distances downstream.

4 THE STATIONARY PROBLEM

Below we shall consider that the plasma may be relativistic, or nonrelativistic and as before we shall neglect gravity and thermal pressure. By $U_p = \gamma V_p/c$ and $U_\varphi = \gamma V_\varphi/c$, we denote the poloidal and azimuthal 4-speeds where V_φ is the azimuthal and V_p the poloidal components of the velocity while γ is the Lorentz factor of the plasma. In the following subsection we review the basic quantities which remain invariant along a poloidal streamline $\psi = const.$ and express momentum balance along such a poloidal streamline. In the next subsection we adopt a new coordinate system for dealing with the transfield equation expressing momentum balance across the poloidal streamlines.

4.1 MHD Integrals

As is well known, the stationary MHD equations admit four integrals. They are:

(α) The ratio of the poloidal magnetic and mass fluxes, $cF(\psi)$

$$cF(\psi) = \frac{B_p}{4\pi\rho V_p}. \quad (9)$$

(β) The total angular momentum per unit mass $L(\psi)$,

$$rcU_\varphi - cFrB_\varphi = L(\psi). \quad (10)$$

(γ) The corotation frequency $\Omega(\psi)$ in the frozen-in condition

$$cU_\varphi B_p - cU_p B_\varphi = r\gamma B_p \Omega(\psi). \quad (11)$$

(δ) The total energy $c^2 W(\psi)$ in the equation for total energy conservation,

$$\gamma c^2 - cF(\psi)r\Omega(\psi)B_\varphi = c^2 W(\psi). \quad (12)$$

4.2 The transfield equation in the coordinates (ψ, η).

Momentum balance across the poloidal fieldlines is expressed by the transfield equation which determines and their shape. This is a rather complicated nonlinear partial differential equation of mixed elliptic/hyperbolic type. For analysing the behaviour of the plasma at large distances, it occured to us that it is rather convenient to work with this transfield equation in an orthogonal curvilinear coordinate system (ψ, η) formed by the tangent to the poloidal magnetic field line $\hat{\eta} = \hat{p}$ and the first normal towards the center of curvature of the poloidal lines, $\hat{\psi} = \nabla\psi/|\nabla\psi|$ (Sakurai, 1990). A geometrical interval in these coordinates can be expressed as

$$(d\mathbf{r})^2 = g_\psi^2 d\psi^2 + g_\eta^2 d\eta^2 + r^2 d\varphi^2, \quad (13)$$

where g_ψ, g_η are the corresponding line elements or components of the metric tensor.

If T^{ij} is the energy-momentum tensor of the plasma flow ($\rho\vec{V}$) and electromagnetic field ($\vec{E}, \vec{B}$) (Landau & Lifshitz 1975), the equation $\partial T^{\psi k}/\partial x^k = 0$ (with covariant derivatives) has the following form in the coordinates (ψ, η),

$$\frac{\partial}{\partial\psi}\left[\frac{B^2 - E^2}{8\pi}\right] - \frac{1}{r}\frac{\partial r}{\partial\psi}\left[\rho V_\varphi^2 - \frac{B_\varphi^2 - E^2}{4\pi}\right] - \frac{1}{g_\eta}\frac{\partial g_\eta}{\partial\psi}\left[\rho V_p^2 - \frac{B_p^2 - E^2}{4\pi}\right] = 0. \quad (14)$$

The first term in this equation is the gradient of the pressure of the electromagnetic field, while the second is the sum of the inertial terms due to the motion of the plasma in the azimuthal direction and also due to the tension of the toroidal magnetic field. To better understand the physical meaning of the last term, note that since $\hat{\eta}$ is perpendicular to $\hat{\psi}$ we have,

$$\frac{1}{g_\eta}\frac{\partial g_\eta}{\partial\psi} = \frac{1}{rR_c B_p}, \quad (15)$$

where R_c is the radius of curvature of the poloidal magnetic field lines, with R_c positive if the center of curvature is in the domain between the line and the axis of rotation and negative in the opposite case.

With this expression, Eq. (14) becomes,

$$\frac{\partial}{\partial\psi}\left[\frac{B_p^2}{8\pi}\right]+\frac{1}{8\pi r^2}\frac{\partial}{\partial\psi}\left[r^2(B_\varphi^2-E^2)\right]-$$

$$\frac{1}{4\pi r}\frac{\partial r}{\partial\psi}\frac{U_\varphi^2 B_p}{U_p F(\psi)}-\frac{[U_p-F(\psi)(1-(r\Omega/c)^2)B_p]}{4\pi r R_c F(\psi)}=0\,. \quad (16)$$

From this equation, it may be seen that the last term is the sum of the inertia of plasma and fields, connected with the motion of the plasma and Poynting flux along the poloidal field line and tension of the poloidal field line.

4.3 The transfield equation for nonrelativistic plasmas with gravity and thermal pressure included

For completeness of the picture we present briefly here the transfield equation for a nonrelativistic plasma flow to demonstrate that our method of solution of the stationary problem in the hyperbolic region can be applied directly to this case too. The energy momentum conservation equation in the presence of gravity in the nonrelativistic limit is modified as $\partial T^{\psi k}/\partial x^k=-\rho\partial\Phi/\partial x^\psi$, where $T^{\psi k}$ is again the energy-momentum tensor, $\Phi=-GM/R$ is the gravitational potential of the star with mass M and G is the gravitational constant. This equation has the following form in our curvilinear coordinates if some thermal pressure P is also included,

$$\frac{\partial}{\partial\psi}\left[P+\frac{B^2}{8\pi}\right]-\frac{1}{r}\frac{\partial r}{\partial\psi}\left[\rho V_\varphi^2-\frac{B_\varphi^2}{4\pi}\right]-$$

$$\frac{1}{g_\eta}\frac{\partial g_\eta}{\partial\psi}\left[\rho V_p^2-\frac{B_p^2}{4\pi}\right]=-\rho\frac{\partial\Phi}{\partial\psi}\,. \quad (17)$$

All other equations, describing the flow of plasma along field lines will be the same except the energy conservation equation which is modified as follows

$$\frac{V^2}{2}+\frac{\delta}{\delta-1}\frac{P}{\rho}+\Phi-cF(\psi)r\Omega(\psi)B_\varphi=W(\psi)c^2\,. \quad (18)$$

where δ is the polytropic index of the plasma.

5 THE SOLUTION IN THE FAR ZONE.

It is convenient to solve the transfield equation in the system of the curvilinear coordinates introduced above. The unknown variables are $z(\eta,\psi)$ and $r(\eta,\psi)$. Therefore we need to know the quantities g_η, g_ψ, r_ψ, z_ψ, r_η, z_η, where $r_\eta=\partial r/\partial\eta$, $z_\eta=\partial z/\partial\eta$, $r_\psi=\partial r/\partial\psi$, $z_\psi=\partial z/\partial\psi$.

First, the metric coefficient g_η is obtained from the transfield equation (14),

$$g_\eta=\exp\Big(\int_0^\psi G(\eta,\psi)d\psi\Big)\,, \quad (19)$$

where

$$G(\eta,\psi)=$$

$$\frac{\frac{\partial}{\partial\psi}\left[\frac{1}{8\pi}(B^2-E^2)\right]-\frac{1}{r}\frac{\partial r}{\partial\psi}\left[\rho V_\varphi^2-\frac{1}{4\pi}(B_\varphi^2-E^2)\right]}{\left[\rho V_p^2-\frac{1}{4\pi}(B_p^2-E^2)\right]}\,, \quad (20)$$

for a cold plasma. For a nonrelativistic flow with finite thermal pressure and gravity the function G will have the form

$$G(\eta,\psi)=$$

$$\frac{\frac{\partial}{\partial\psi}\left[\frac{1}{8\pi}B^2+P\right]+\frac{\partial}{\partial\psi}\Phi-\frac{1}{r}\frac{\partial r}{\partial\psi}\left[\rho V_\varphi^2-\frac{1}{4\pi}B_\varphi^2\right]}{\left[\rho V_p^2-\frac{1}{4\pi}B_p^2\right]}\,. \quad (21)$$

The lower limit of the integration in Eq. (19) is chosen to be 0 such that the coordinate η is uniquely defined. In this way η coincides with the coordinate z where the surface of constant η crosses the axis of rotation.

Second, the metric coefficient g_ψ is given in terms of the magnitude of the poloidal magnetic field by,

$$g_\psi=\frac{1}{rB_p}\,. \quad (22)$$

To obtain the expressions of r_ψ, z_ψ, r_η, z_η we may use the orthogonality condition

$$r_\eta r_\psi+z_\eta z_\psi=0\,, \quad (23)$$

and also the fact that they are related to the metric coefficients g_η and g_ψ as follows,

$$g_\eta^2=r_\eta^2+z_\eta^2\,, \quad (24)$$

$$g_\psi^2=r_\psi^2+z_\psi^2\,. \quad (25)$$

Thus, by combining the condition of orthogonality (23) and equations (24) and (25) the remaining values of r_η, z_η are obtained,

$$r_\eta=-\frac{z_\psi g_\eta}{g_\psi}\,, \quad (26)$$

$$z_\eta=\frac{r_\psi g_\eta}{g_\psi}\,. \quad (27)$$

with g_η calculated by the expression (19). For the numerical solution of the system of equations (26 - 27) a two step Lax-Wendroff method is used on a lattice with a dimension equal to 1000.

Equations (26 - 27) should be supplemented by appropriate boundary conditions on some initial surface of constant η. The equations for r_ψ, z_ψ defining this initial surface in cylindrical coordinates are as follows

$$\frac{\partial r}{\partial\psi}=\frac{B_z}{rB_p^2}\,, \quad (28)$$

$$\frac{\partial z}{\partial\psi}=-\frac{B_r}{rB_p^2}\,. \quad (29)$$

We need to specify on this surface the integrals $F(\psi), L(\psi), \Omega(\psi)$ and $W(\psi)$ as the boundary conditions for the initial value problem. To specify the initial surface of constant η and the above integrals, we use the results of the solution of the problem in the nearest zone when a stationary solution is obtained for the time-dependent problem.

6 RESULTS IN THE NEAREST ZONE FOR UNIFORM ROTATION, $\Omega(\psi)=\Omega_O$

As the star starts rotating, in the initially radial magnetosphere an MHD wave propagates outwards carrying the

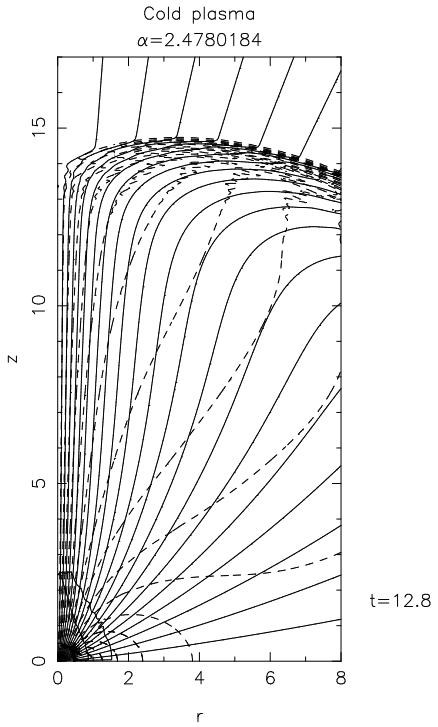

Figure 1. *A near zone snapshot on the poloidal plane (Z, r) from the simulation showing the change of the shape of the poloidal magnetic fieldlines from an initially uniform with latitude radial monopole and before a stationary state is reached. Distances are given in units of the Alfvén radius R_a and time in units of the Alfvén crossing time $t_a = R_a/V_a$*

effect of the rotation and deflecting the fieldlines polewards by the Lorentz force (Fig. 1).

At times sufficiently long after the shock wave has reached the end boundary of the simulation ($t >> 1$), a final equilibrium state is reached (Figs. 3). In this stationary state, the poloidal magnetic field and the plasma density are increased along the axis because of the focusing of the field lines towards the pole.

In Figs. (3) the distances are given in units of the initial Alfvenic radius R_a. Thick lines indicate Alfvén and fast critical surfaces while thin lines the poloidal magnetic field. At $t = 0$ the Alfvén surface is spherical at $R = 1$. Dotted lines indicate poloidal currents.

With the velocity maintaining the constant initial value V_o along the Z-axis, the ratio B_p/ρ remains constant along this axis ($\psi = 0$). As a result, the Alfvén speed at a given point of the Z-axis, $V_A = B_p/\sqrt{4\pi\rho}$, increases as the square root of the density increases there because of focusing. It follows that the Alfvén transition at $R_A(\theta = 0)$ occurs further downstream where $V_o(R_A) = V_A(R_A)$, i.e., at $R_A(\theta = 0) > 1$. As we move meridionally off the polar axis toward the equator on the other hand, the bulk flow speed is increased because of the magnetocentrifugal acceleration; it thus hits the Alfvén value earlier than it does on the axis, i.e., $V(\theta) = V_A(\theta)$, at $R_A(\theta) < R_A(\theta = 0)$. Finally, on the equator the flow speed increases rapidly with the result that the flow becomes much earlier super Alfvénic there in comparison to the polar axis. The degree of elongation of the

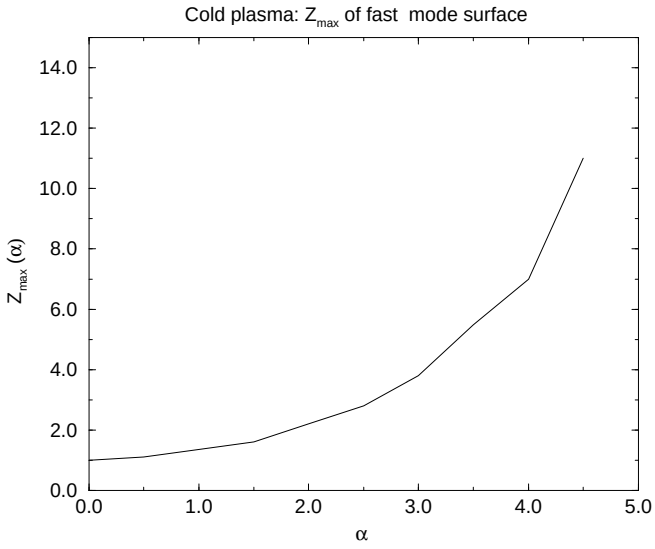

Figure 2. *Maximum height Z_{max} of fast critical surface as a function of α, in units of the base radius R_a.*

Alfvén surfaces along the symmetry axis increases with the value of α.

The behaviour of the fast surface has similarities and differences with the shape of the Alfvén surface. First, both these critical surfaces coincide at $\theta = 0$. As we move meridionally off the polar axis toward the equator on the other hand, their shape becomes different. This is due to the contribution of the azimuthal field, since in this case of cold plasma $V_f^2 = (B_p^2 + B_\phi^2)/4\pi\rho$. Thus, for small colatitudes θ, V_f increases due to the contribution of B_ϕ while also V slightly increases because of the magnetocentrifugal acceleration. However, initially V_f increases faster and therefore the fast transition is postponed further downstream. At larger θ however, the competing flow speed V increases faster than V_f does and the fast transition occurs closer and closer to the origin.

The dependance of the maximum height Z_{max} of the fast critical surface as a function of α is interesting too (Fig. 2). As α increases, Z_{max} increases rapidly. That means that for sufficiently fast rotators with $\alpha \geqslant 5$, Z_{max} goes to infinity and the flow may stay sub-fast all the way to large distances. This result may have some important implications in the general theory of MHD winds. It clearly indicates that a super-fast stationary solution may not be obtained for all sets of parameters. For large α no super-fast stationary state is found and thus the equilibrium is vulnerable to instabilities. Such a situation may take place, for example, in young rapidly rotating stars. Outflows from classical accretion disks (Shakura & Sunyaev 1973) are also expected to have such large values of α, since the Alfvén and sound speeds in such disks are much smaller than their respective Keplerian speed. Thus, since $V_a \sim V_s << V_K$ and $r_a > r_K$, we have

$$\alpha = \frac{\Omega r_a}{V_a} >> \frac{\Omega r_K}{V_K} \approx 1\,.$$

It follows that outflows from rapidly rotating stars and

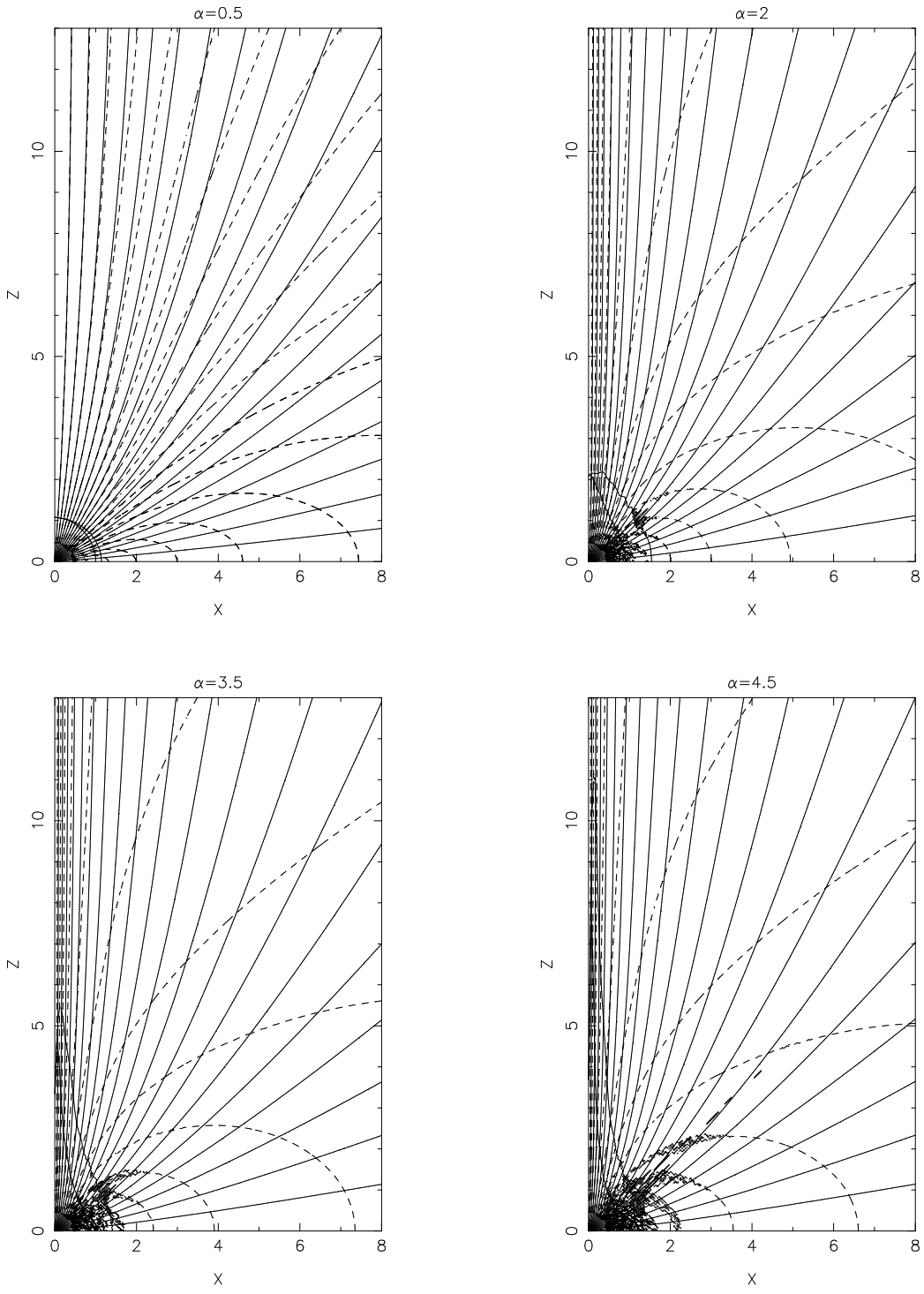

Figure 3. Sequence of shapes of the poloidal field lines by increasing the magnetic rotator parameter α from $\alpha = 0.5$ (solar wind type slow magnetic rotator) to $\alpha = 4.5$ (fast magnetic rotator). The initial nonrotating monopole magnetic field has a spherical Alfvén surface located at $R = 1$ and all distances are given in units of the Alfvén radius R_a with the base located at $R = 0.5$. Dotted lines indicate poloidal currents. Thick lines indicate Alfvén and fast critical surfaces. At $t = 0$ the Alfvén surface is spherical at $R = 1$.

thin classical accretion disks may rather produce jets with characteristics which qualitatevely differ strongly from those of laminar jets usually discussed in the literature. This result is certainly obtained under the simplifying assumptions of the present study, and further investigations are necessary to explore the possibilities which may arise in this regime of outflow. Up to now all numerical simulations avoided this problem by artificially taking $\alpha \sim 1$ in order to obtain a stationary solution (Romanova et al 1997), or, no stationary solution was obtained at all (Ouyed & Pudritz 1997, see Fig. 8 in this work). Fig. (3) then may indicate why no simulation has succeeded to produce stationary supersonic jet from classical accretion disks up to now (Ferreira, 1997).

7 RESULTS IN THE FAR ZONE

The characteristics of magnetized outflows at large distances from the central object have been studied by Heyvaerts & Norman (1989), Chiueh et. al. (1991) and Bogovalov (1995). These studies have concluded that a stationary axisymmetrically rotating object ejecting magnetized plasma always produces a jet collimated exactly along the axis of rotation, *if* the following conditions are satisfied:
1. The flow is nondissipative.
2. The angular velocity of rotation is nonzero everywhere (actually, if $\Omega = 0$ on some field lines, the same conclusion remains valid).
3. The total magnetic flux reaching infinity in any hemisphere of the outflow is finite.
4. The polytropic index of the plasma $\delta > 1$.
In such an outflow the density of the poloidal electric current is nonzero in the region of the collimated flow. Conversely, in the region of noncollimated field lines the density of the poloidal electric currents equals to zero. This condition can be expressed by the constancy of the quantity $r^2\Omega(\psi)B_p/U_p$, which we shall call the Heyvaerts-Norman integral.

7.1 Efficiency of the magnetic rotator

In the Weber & Davis (1967) model of a magnetized equatorial wind the terminal equatorial speed is superfast with the fast mode surface placed at some finate distance from the star. If the initial velocity of a cold plasma is equal to zero on the surface of the star, the fast critical point is at infinity and we obtain the so-called Michel's (1969) minimum energy solution. This solution is valid when the monopole-like poloidal magnetic field is slightly disturbed by the plasma. In this case the asymptotic speed at infinity on the equator is $V_\infty = (3/2)V_a$, while the *total* specific angular momentum in the system in units of R_aV_o is, $L = \Omega r_a^2/R_aV_o$. We recall that R_a is the radius of the initial spherical Alfvén surface while r_a is the Alfvenic radius on the equator at a given angular velocity. An important physical quantity in magnetized outflows is the magnetic rotator energy, E_{MR}, the product of the total specific angular momentum and Ω. The basal Poynting energy defined as the ratio of the Poynting flux density S_z per unit of mass flux density ρV_z is approximately equal to $E_{\rm MR}$ *if* at the base of the outflow the radius of the jet is much smaller than the Alfvén radius and also the Alfvén number there is negligibly small.

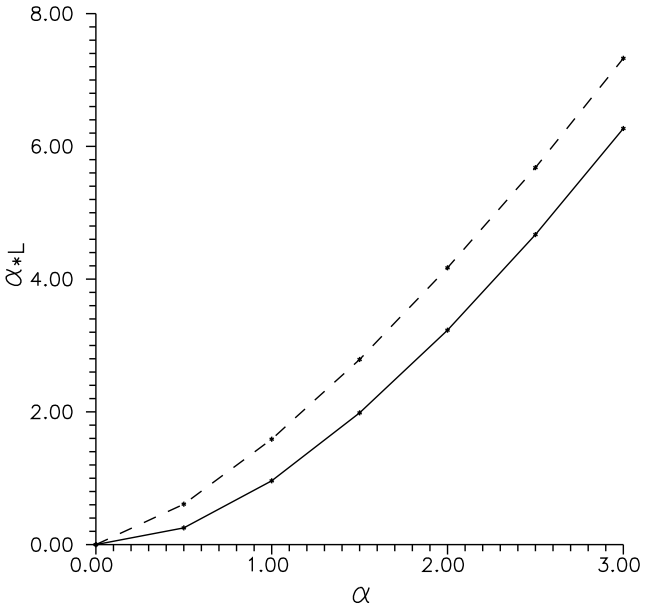

Figure 4. *For a magnetic rotator we plot the rotational losses αL per particle, as a function of α (solid line). For comparison, the corresponding rotational losses for Michel's minimum energy solution are also plotted (dashed line).*

The energy losses of the magnetic rotator per particle in units of V_o^2 are

$$\frac{E_{\rm MR}}{V_o^2} = \frac{\Omega^2 r_a^2}{V_o^2} = \alpha L\,. \qquad (30)$$

This formula is widely used in the theory of the rotational evolution of stars. But the parameter α goes to ∞ in Michel's minimum energy solution. The plasma is strongly collimated under this condition and therefore Michel's solution is not valid. In this case it is important to know how strongly the effect of collimation affects those frequently used Michel's energy losses. The energy losses αL per particle on the equator for Michel's monopole-like solution and our calculations are compared in Fig. 4.

The decceleration rate in our solution is less than in Michel's solution. This is due to the collimation of the plasma. The poloidal magnetic field near the equator decreases and it leads to a reduction of the decceleration rate.

It is interesting that in spite of the decrease of the decceleration rate the terminal velocity of the plasma near the equator increases in our solution. The terminal speed V_∞ as a function of α is plotted in Fig. (5). The terminal velocity is calculated on the equator at the dimensionless distance X=500. For the case of a fast magnetic rotator (Michel 1969), the dependance of V_∞ on α is,

$$\frac{V_\infty}{V_o} = \frac{1}{V_o}\left(\frac{\Omega^2 R_a^4 B_a^2}{\dot{M}}\right)^{1/3} = \alpha^{2/3}\,,$$

i.e., it goes like $\alpha^{2/3}$. This increase of the terminal velocity on the equator in comparison to that in Michel's solution is due to the collimation of the plasma. In the ollimated flow there exist strong gradients of the toroidal magnetic field which additionally accelerate plasma. This means that in

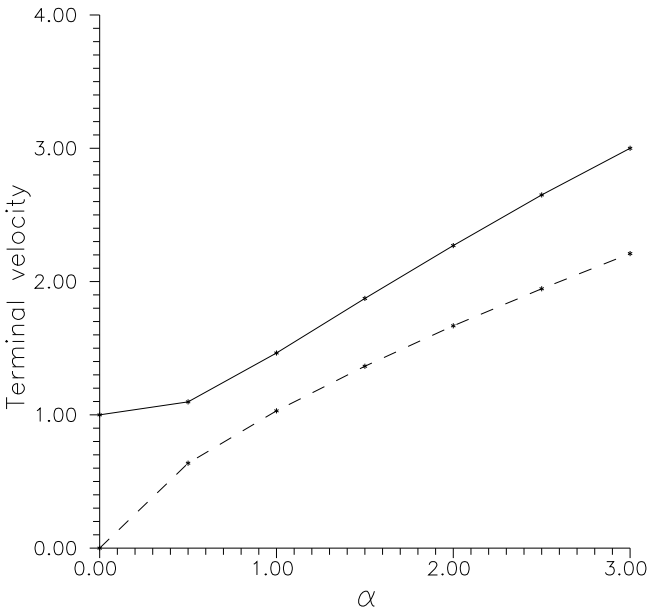

Figure 5. *The terminal velocity V_∞/V_o as a function of α (solid line). For comparison, the corresponding terminal speed in Michel's minimum energy solution is also plotted (dashed line).*

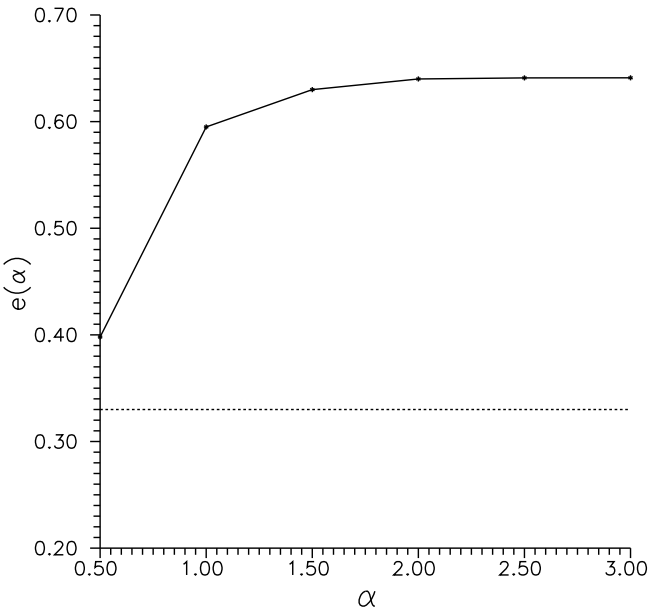

Figure 6. *Efficiency e of the magnetic rotator as a function of α (solid line). For comparison, Michel's solution has $e = 1/3$ (dotted line).*

collimated ouflows we have a more effective acceleration of the plasma by the magnetic rotator.

The efficiency e of the magnetic rotator in transforming part of the base Poynting flux to poloidal kinetic energy at infinity is measured as the difference of the poloidal kinetic energies at infinity and at the base normalized to the total energy E (in units of V_o^2). The poloidal kinetic energy at infinity in Michel's solution in units of V_o^2, E_∞^{pol} is

$$E_\infty^{pol} = \frac{E}{3} = \frac{\Omega^2 r_a^2}{3V_o^2}\,,$$

or,

$$E_\infty^{pol} = \frac{1}{3}\frac{\Omega {r_o}^2}{V_o}\left(\frac{r_a}{r_o}\right)^2 = \frac{1}{3}\alpha^2\left(\frac{r_a}{r_o}\right)^2 = \frac{1}{3}\alpha L\,.$$

The efficiency e is plotted in Fig. (6) for our solution and (solid) and for Michel's solution (dashed). We see that due to collimation, the magnetic rotator becomes a very effective machine for plasma acceleration.

7.2 The radius of the jet

The dependence of the magnitude of the poloidal magnetic field and density on the cylindrical distance r becomes especially simple if we assume for convenience that the following additional conditions are met in the jet, namely that the integrals $W(\psi), L(\psi), F(\psi), \Omega(\psi)$ and the terminal velocity V_j are constants and do not depend on ψ and also that $V_j \gg V_a(0)$, where $V_a(0)$ is the Alfvenic velocity on the axis of rotation. In such a case, Eqs. (16) - (28) give an approximate estimate of the dependence of the magnetic field on r (Bogovalov 1995),

$$\frac{B_p(r)}{B_p(0)} = \frac{\rho(r)}{\rho(0)} = \frac{1}{(1+(r/R_j)^2)}, \qquad (31)$$

where R_j is the radius of the core of the jet

$$R_j = \sqrt{(1+\frac{C_s(0)^2}{V_a(0)^2})}\frac{\gamma V_j}{\Omega}, \qquad (32)$$

with $C_s(0)$ the sound velocity along the jet's axis and $B_p(0)$, $\rho(0)$ the magnetic field and the density of the plasma on the axis of the jet, respectively. It is evident that the poloidal magnetic field and the density remain practically constant up to distances of order R_j and then decay fast like $1/r^2$ outside the jet's core.

Among the main goals of the present paper is the verification of these conclusions, together with the investigation of the process of jet formation and the development of methods for the calculation of the characteristics of the plasma in the jet.

In Fig. (7) the poloidal and azimuthal components of the magnetic field are plotted together with the magnetic flux enclosed by a cylindrical distance X. The poloidal magnetic field $B_p(X)/B_o$ (solid line) is given in units of its reference value B_o, corresponding to the magnetic field at the symmetry axis $r = 0$ and some reference height $Z_o = 60825$ for $\alpha = 0.5$ and $Z_o = 5000$ for $\alpha = 3$. The asymptotic regime of the jet is achived at these distances. The intensity of the poloidal magnetic field drops dramatically by more than 50% with respect to its value at the axis $X = 0$ within a distance of the order of the collimation radius $X_j = 1/\alpha$. The dashed curve gives the analytically predicted solution for the poloidal magnetic field $B_p(X)/B_o$, Eq. (31). Apparently, for small values of α there is a good agreement between the calculated and analytically predicted values of the poloidal magnetic field. For $\alpha = 3$ the agreement between the analytical prediction and numerical calculations is worse than for $\alpha = 0.5$. This is natural because the condition $V_j \gg V_a(0)$ under which the analytical prediction is valid becomes not so good fulfilled for $\alpha = 3$ as for $\alpha = 0.5$.

The strength of the azimuthal magnetic field $B_\phi(X)/B_o$ (dots) obtains a maximum value at the radius X_j. For

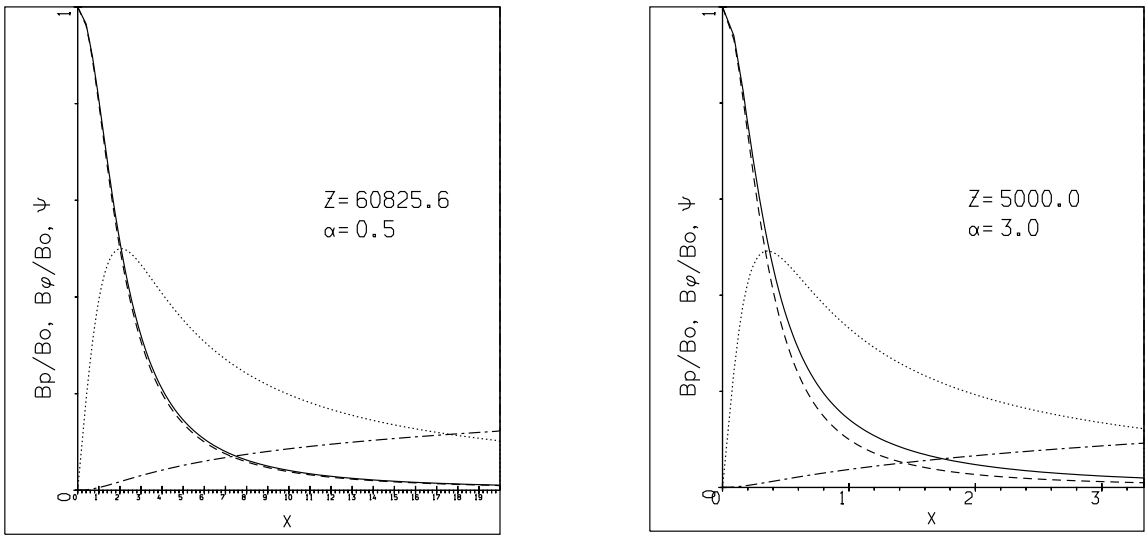

Figure 7. *Variation with the dimensionless cylindrical distance X of the enclosed magnetic flux $\psi(X)$ (dot-dashes), strength of the azimuthal magnetic field $B_\phi(X)/B_o$ (dots) and poloidal magnetic field $B_p(X)/B_o$ (solid) for a slow magnetic rotator $\alpha = 0.5$ and a faster magnetic rotator $\alpha = 3$. With dashes the analytically predicted solution for the poloidal magnetic field $B_p(r)/B_o$ is also shown.*

$X < X_j$ we have approximately conditions similar to those corresponding to a uniform current density wire and therefore $B_\phi \propto X$. On the other hand, for $X > X_j$, conditions like those existing outside of a uniform current density wire exist and therefore $B_\phi \propto X^{-1}$.

7.3 The Heyvaerts & Norman enclosed current

The enclosed electric current by a poloidal field line $\psi = const.$ is plotted in Fig. (8a) for $\alpha = 3$. We may distinguish three regimes. Close to the axis, $0 < \psi < 0.1$ the current increases with ψ since there we have conditions similar to those corresponding to some uniform current density wire. A new regime appears when we are outside the collimated region where the enclosed current reaches a plateau, $0.1 < \psi < 0.5$. We shall call this regime the Heyvaerts-Norman regime, since there we have conditions similar to those existing outside a uniform current density wire ($XB_\phi = const.$), a situation described by Heyvaerts & Norman (1989). Finally, a third domain exists in $0.5 < \psi < 1$ where again the enclosed current increases. It seems that this contradicts the expected behaviour, but as we show below it is due to very slow decrease of this part of the current and we do not achieve final asymptotics.

7.4 Logarithmic collimation asymptotically

One may use the coordinates (η, ψ) to show the distribution of the electric currents, Figs. (8b). In this space, $\psi = 0$ corresponds to the symmetry axis $X = 0$, $\psi = 1$ to the equator and $\eta = 0$ approximately to the source surface, while a poloidal fieldline corresponds to some vertical line $\psi = const.$ Fig (8b) demonstrates that there is an electric current near the axis. Then the Heyvaerts & Norman region of constant XB_φ is formed. And finally the region where XB_φ increases is observed. It is important that the excess of the electric current in this last region decreases with η. But this decrease occurs in a logarithmic scale. The solution goes to its asymptotic form, but this is done very slowly, in a logarithmic scale. This behavior can be demonstrated also by a simple analysis of the transfield equation.

In a supersonic flow, the motion of every parcel of plasma is controlled by the initial conditions and the forces affecting the plasma. Here we are interested in the collimation process in the region of radially expanding field lines. In this region forces due to the poloidal magnetic field and the inertia of the plasma due to motion in the azimuthal direction can be neglected in the transfield equation in comparison to forces arising from the toroidal magnetic field. The terms $B_p^2/8\pi$ and ρV_φ^2 can be neglected since they drop with distance r as $1/r^4$, while the terms corresponding to the azimuthal magnetic field B_φ^2 drop as $1/r^2$. Then, the transfield equation Eq. (16) is simplified as follows,

$$\frac{1}{8\pi r^2}\frac{\partial}{\partial\psi}(rB_\varphi)^2 - \frac{U_p}{4\pi r R_c F(\psi)} = 0. \tag{33}$$

It may be seen from this equation that the curvature radius of a field line of the poloidal magnetic field is defined by the tension of the toroidal magnetic field. Let us estimate how the curvature radius of the poloidal magnetic field changes with distance assuming for simplisity that the poloidal magnetic field expands radially and hardly depends on the polar angle θ near equator. At large distances, the frozen in condition gives for the electric current

$$rB_\varphi = -\frac{r^2\Omega B_p}{V_p}. \tag{34}$$

Inserting this in (33) and assuming that the dependence of B_p on θ is weak, we get

$$\frac{2\cos\theta B_p\Omega^2}{V_p^2} = \frac{V_p}{rR_cFc}. \tag{35}$$

The curvature radius of the field line is defned by the equation

$$R_c = \frac{dl}{d\theta}, \tag{36}$$

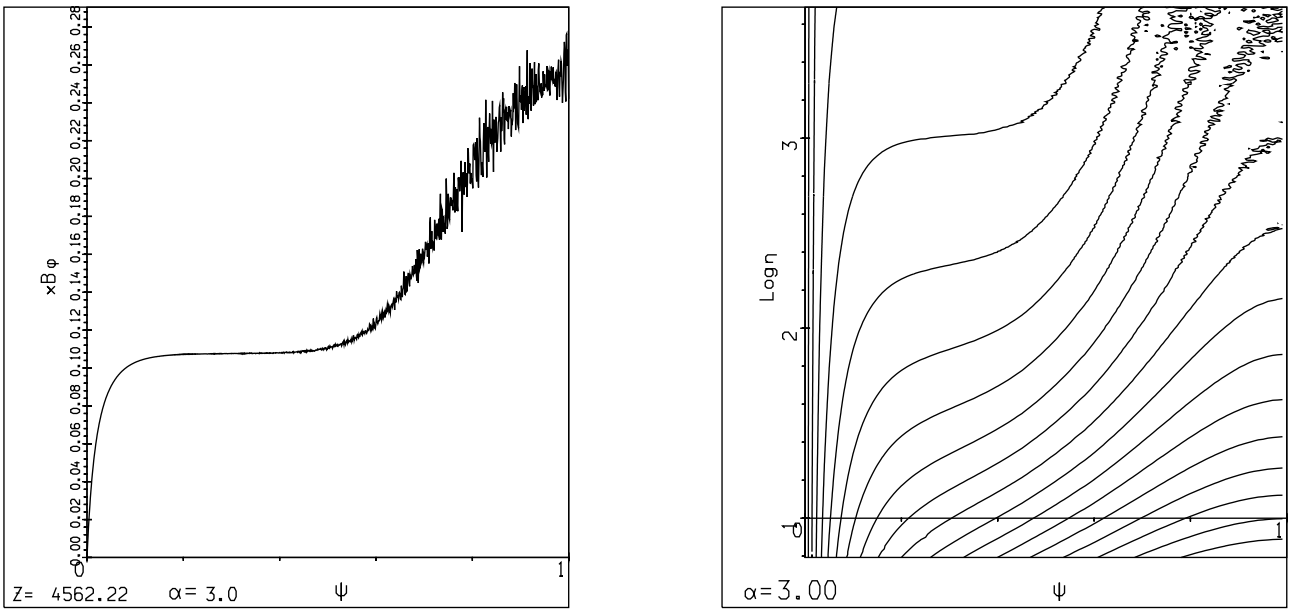

Figure 8. *For $\alpha = 3$, in (a) it is plotted the enclosed electric current XB_ϕ by each poloidal field line ψ and in (b) the iso-current contours in the space of (η, ψ).*

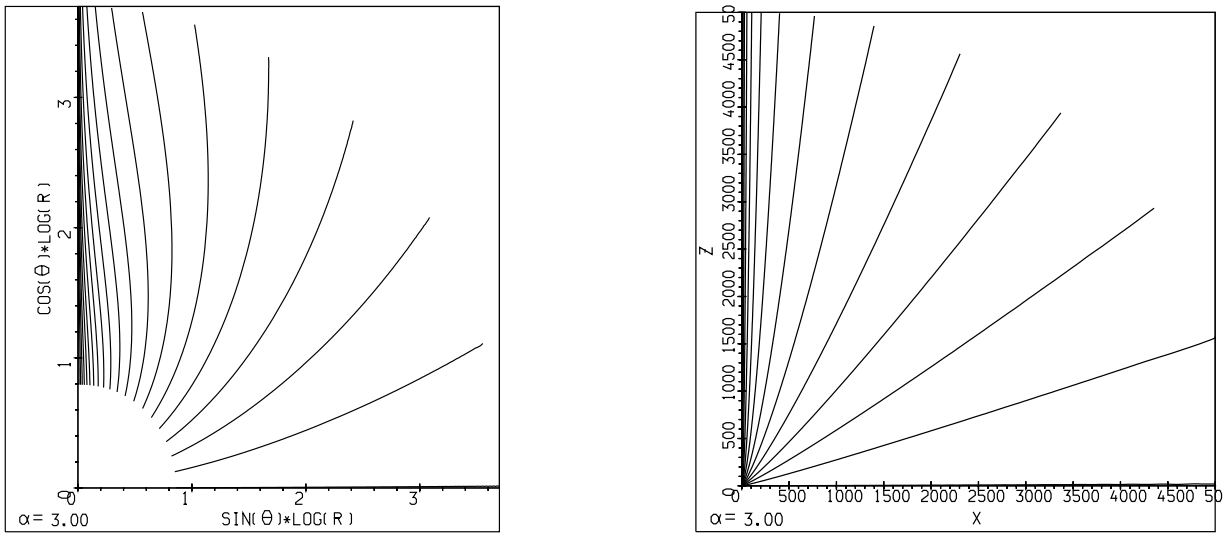

Figure 9. *Shape of the poloidal magnetic field lines for a magnetic rotator parameter $\alpha = 3$ plotted up to a radius 5000 times the initial base radius. In (a) the poloidal field lines are plotted in a logarithmic scale, and give the erroneous impression that all fieldlines are focused towards the system's symmetry axis. In the linear scale of Fig. (b) however, a cylindrical jet is formed around the symmetry axis while all other field lines go to straight asymptotes which fill all space.*

where dl is the element of the length of the fied line. Since to a first approximation $dl = dR$, where R is the spherical distance to the center of the rotating object, we get for the equation of a field line,

$$\frac{d\theta}{dR} = \frac{cFB_pR^2\Omega^2}{RV_p^3}\sin 2\theta\,. \tag{37}$$

For a radially expanding magnetic field B_pR^2 is constant along a magnetic field line. Therefore, the turn angle of the field line $\Delta\theta$ depends logarithmically on R,

$$\Delta\theta = \frac{cFB_p(R\Omega)^2\sin 2\theta}{V_p^3}\ln\frac{R}{R_0}, \tag{38}$$

where R_0 is the initial distance. According to (34) the change

of the electric current enclosed by a field line is connected with the divergence of the poloidal magnetic field from the purely radial shape. To have variation of rB_φ with ψ it is necessary to turn some field lines at some angle. Such a turn occurs at the exponentially large distances defined by the expression

$$R = R_0 \exp\left(\frac{V_p^3 \Delta\theta}{cFB_p(R\Omega)^2 \sin 2\theta}\right) > R_0 \exp \frac{\Delta\theta \tan\theta}{2}. \quad (39)$$

because for the super fast magnetosonic plasma we have

$$V_p > cFB_\varphi^2/B_p, \quad (40)$$

which taking into account (34) can be rewritten as $V_p^3 > cFB_p r^2\Omega^2$. In other words, the magnitude of the exponent in Eq. (39) is larger than $\Delta\theta \tan\theta/2$, a large number near the equator. Apparently, two points at small angular distance $\Delta\theta$ on the same fieldline have exponentially large radial distances R_0 and R from the origin. This explains the picture we obtain in the numerical solution and agrees with earlier results obtained by Eichler (1993) and by Tomimatsu (1994).

In the logarithmic scale of Figs. (9a) the impression one may get is that all poloidal fieldlines are focused towards the symmetry axis. Such a figure was produced in Sakurai (1985). However, this way of plotting the shape of the poloidal streamlines is a deceiving about the asymptotical shape of the magnetosphere which is different, as seen in the linear scale of Fig. (9b). In this plotting it is clear that the geometry of the poloidal field lines is such that a cylindrical core (the jet) is formed around the symmetry axis with a width of the order of the base radius, but all other field lines go to straight asymptotes filling all space.

8 ACCRETION DISK-LIKE ROTATION, $\Omega = \Omega(\psi)$.

An analysis of the asymptotical behaviour of MHD outflows in Bogovalov (1995) shows that a discontinuity in the total electric current is formed on the equator for outflows from astrophysical objects having a magnetic field directed in opposite directions in the upper and lower hemispheres. In a pure monopole-like magnetic field the electric current leaves the star in the upper hemisphere and returns back in the lower hemisphere. In such a magnetosphere the total electric current is continuous on the equator. But already in the split monopole model where the magnetic field has opposite directions in the upper and lower hemispheres, the closure of the electric circuit occurs along the equator so that on the equator $XB_\phi = 0$. This means that the total electric current flowing in the upper or lower hemispheres is equal to zero. On the other hand, according to Bogovalov (1995) the magnitude of XB_ϕ is not equal to zero on all field lines of the supersonic flow where $\Omega \neq 0$. This means that the function $XB_\phi(\psi)$ shown in Fig. (8a) has actually a discontinuity at the point $\psi = 1$ (on the equator) for the split monopole solution. This is the usual MHD contact discontinuity between the flows in the upper and lower hemispheres with the magnetic field equal to each other in magnitude but with different directions. It is important to check the validity of this conclusion for a pure monopole-like magnetic field.

In the following, we shall investigate the process of the formation on the equator of such a discontinuity in the total electric current, in the ideal MHD approximation. For this purpose, we take the rotation of the star such that the total electric current which flows in each of the upper or lower hemispheres to be independently equal to zero. For example, this happens with a differential law of rotation wherein $\Omega(\psi) = 0$ on the equator and the fieldline on the equator does not rotate. This guarantees that $XB_\phi = 0$, everywhere on the equator.

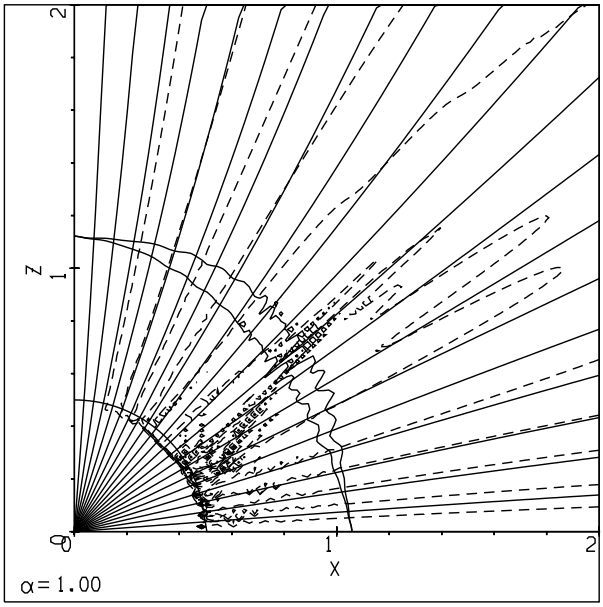

Figure 10. *Shape of the poloidal magnetic field lines in the near zone of a differentially rotating magnetic rotator with $\alpha = 1$: the field lines focus towards the pole and the equator.*

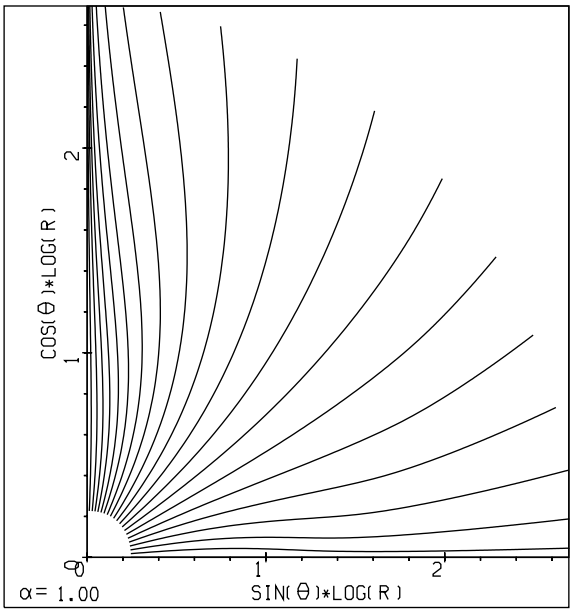

Figure 11. *Shape of the poloidal magnetic field lines for a differentially rotating magnetic rotator with $\alpha = 1$, plotted in a logarithmic scale up to a radius 1000 times the initial base radius.*

In this work we took the simplest law of rotation

$$\Omega(\psi) = \alpha(1-\psi)\,. \tag{41}$$

It is worth to pay attention to the fact that that this law of rotation describes qualitatively the rotation of accretion disks where the largest angular velocity is in the inner edge of the disk and the lower one at the outer edge of the disk. The solution of the problem for this differential law of rotation in the nearest zone is shown in Fig. (10).

The most important difference with isorotation is the coincidence of the fast mode and Alfvenic surfaces on the equator. This is simply the consequence of the assumed zero toroidal magnetic field on the equator.

The poloidal magnetic field in the far zone is shown in a logarithmic scale in the next Fig. 11. It is clearly seen in this figure that along with the expected collimation of the flow towards the axis of rotation, there is also a focusing of the flow towards the equator. The explanation of this result is simple. With the assumed differential law of rotation, the largest toroidal magnetic field in the nearest zone is found somewhere at the middle latitudes. The pressure of this toroidal magnetic field pushes the plasma towards the equator and the pole from those mid latitudes.

Fig. (12) shows the formation of a discontinuity in the total electric current near the equator ($\psi = 1$). On the other hand, iso-current contours in Fig. (12b) show that at small η the dependence of XB_ϕ on ψ is that of a smooth function with a maximum placed at $\psi = 0.5$. This maximum moves to the equator as η increases and finally the distribution of XB_ϕ is similar to the one for an isorotation as that shown in Fig. 8, with the exception of a discontinuity formed near the equator.

9 RELATIVISTIC OUTFLOWS

In this section we discuss briefly the problem of collimation of a relativistic plasma. This relativistic version of the problem under consideration differs from the nonrelativistic one only in the modification of the function $G(\eta, \psi)$. In the relativistic case, the terms with the electric field play an important role. To specify the boundary conditions in the super fast magnetosonic region we will use the approximate solution obtained in Bogovalov (1997) for a relativistic plasma outflow in the nearest zone. In this solution the magnetic flux function is

$$\psi = 1 - cos\theta\,, \tag{42}$$

corresponding to the poloidal magnetic field of a magnetic monopole and

$$B_\varphi = -xB_p\frac{\gamma_0}{U_0}\,, \tag{43}$$

where γ_0 is the initial Lorentz factor of the plasma which is ejected from the surface of the star, U_0 is the initial four-velocity of the outflow, x is the cylindrical distance in units of the light cylinder radius. We assume a uniform rotation of the star,

$$U_p = U_0, \qquad U_\varphi = 0\,, \qquad n(r) = \frac{n_0}{r^2}\,, \tag{44}$$

where n_0 is the density of the plasma on the light cylinder. The solution written above is an approximate one, with corrections in the subfast magnetosonic region of the order σ/γ_0^3, where $\sigma = (B_0^2/4\pi mc^2 n)(R_{star}\Omega/c)^2$ is the Poynting flux per particle at the equator. The fast mode surface in these variables is $r_f = \sqrt{\sigma/\gamma_0}$. This solution is valid under the condition $\sigma/\gamma^3 \ll 1$. To get an idea of the physical parameters it may be useful to recall that for the Crab pulsar we have $\sigma \sim 10^6$, $\gamma_0 \sim 10^3$, and $\sigma/\gamma_0^3 \sim 10^{-3}$.

The boundary conditions in the form of the integrals $W(\psi)$, $L(\psi)$, $\Omega(\psi)$, $F(\psi)$ were specified directly after the fast mode surface and the solution obtained is shown in Fig. (13) for sigma $\sigma = 300$ and $\gamma_0 = 30$. The collimation of the flow in this relativistic case is very weak. To explain this let us estimate the dependance of the radius of curvature of the star on the distance to the star assuming that the magnetic field to a first approximation is the field of the magnetic monopole. At large distances, we can neglect the poloidal magnetic field and the azimuthal rotation of the plasma. In this case the transfield equation becomes,

$$\frac{1}{8\pi x^2}\frac{\partial}{\partial\psi}(x^2(H_\varphi^2 - E^2)) - \frac{(U_p + F(\psi)x^2B_p)}{4\pi x R_c F(\psi)} = 0. \tag{45}$$

It is easy to obtain similarly to the nonrealtivistic case the approximate equation for a field line,

$$\frac{d\theta}{dr} = \frac{\sin 2\theta}{rU_0^2(\frac{U_0}{\sigma} + \sin^2\theta)}. \tag{46}$$

An integration of this equation gives approximately,

$$r = r_f \exp\left[\frac{\Delta\theta U_0^2(\frac{U_0}{\sigma} + \sin^2\theta)}{\sin 2\theta}\right]. \tag{47}$$

where r_f is a lower limit of the integration. It may be seen that a large factor $U_0^3/\sigma \gg 1$ is present in the expression above for small angles $\theta < \sqrt{U_0/\sigma}$ and an even larger multiplier U_0^2 at larger angles. Collimation is firstly expected at small angels $\Delta\theta \sim \theta$. Therefore, the distance at which the jet is formed is

$$r_{coll} = r_f \exp\frac{U_0^3}{2\sigma}. \tag{48}$$

For the parameters used in the calculations $r_{coll} = 3.5 \times 10^{19} r_f$. It is interesting to estimate the distances at which we should expect collimation of the wind from the Crab pulsar. For this pulsar $\sigma = 10^6$ $\gamma_0 = 10^3$ and thus we get $r_{coll} \approx 10^{226}$ cm, a value much larger than the size of the cavity (0.1 pc) formed by the wind before it terminates in the interstellar medium.

This result shows that for parameters typical for radio pulsars there is no collimation of the supersonic plasma at resonable distance. Therefore, the plasma is not accelerated in this region as it was also concluded by Begelman & Li (1994).

10 SUMMARY

The axisymmetric 3-D MHD outflow of plasma from a magnetized and rotating central object is numerically simulated for a wide range of angular velocities of the central star. The simulation of the time-dependent evolution of the flow from some initial state was used to obtain finally a stationary

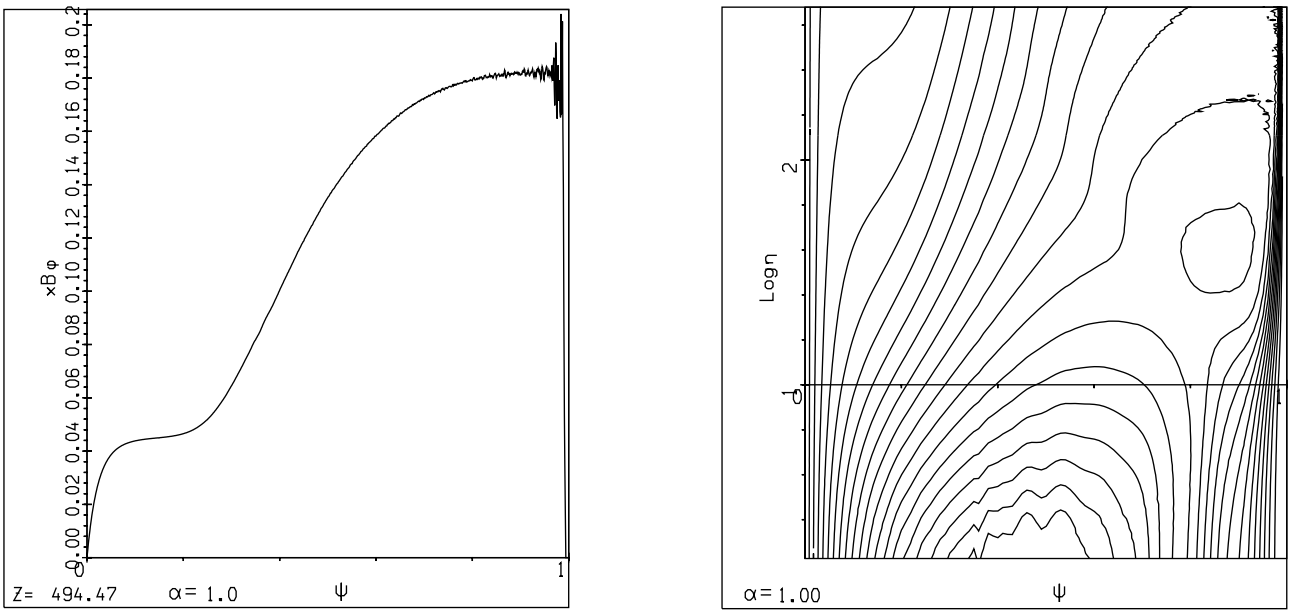

Figure 12. *For a differentially rotating magnetic rotator with $\alpha = 1$, in (a) it is plotted the enclosed electric current XB_ϕ by each poloidal field line ψ and in (b) iso-current contours in the space of (ψ, η).*

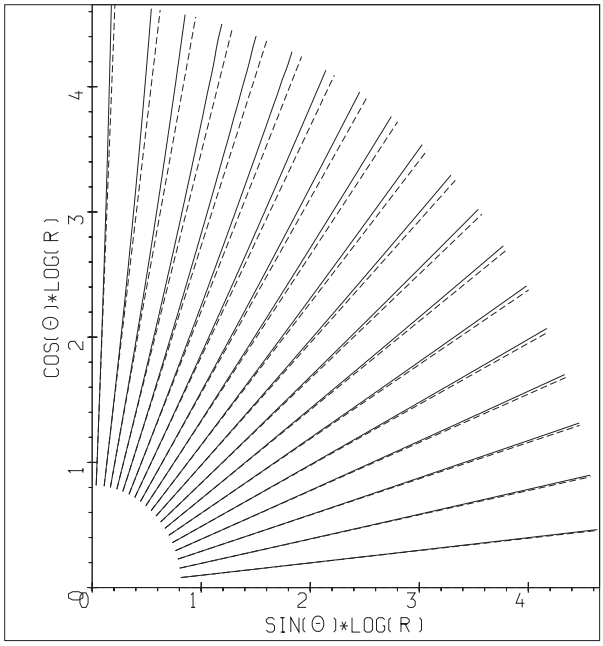

Figure 13. *Shape of the poloidal magnetic field lines (solid) in the far zone of a rotating magnetic rotator ejecting relativistic plasma. Dashed lines show pure radial outflow.*

solution. The model of a non rotating star with a monopole-like magnetic field was taken as the initial state of the magnetosphere. It was found that the obtained stationary final state depends critically on a single parameter only. This parameter α expresses the ratio of the corotating speed at the Alfvén distance to the initial flow speed along the magnetic monopole-like fieldlines. The acceleration of the flow was most effective at the equatorial plane and the terminal flow speed depended linearly on α. Significant flow collimation was found in fast magnetic rotators corresponding to large values of $\alpha > 1$, while very weak collimation occurs in slow magnetic rotators with small values of $\alpha < 1$. Part of the flow around the rotation and magnetic axis is cylindrically collimated while the remaining equatorial part obtains radial asymptotics. The transverse radius of the jet is found to be inversely proportional to α while its density grows linearly with α. For $\alpha > 5$ the magnitude of the speed of the flow in the jet remained below the fast MHD wave speed everywhere. We predict that a regime of nonstationary jet ejections may be possible at such high values of α.

The above results have been obtained under several simplifying assumptions, such as, the neglect of gravity and thermal pressure as well as by taking for the initial magnetosphere a split-monopole configuration. Despite those assumptions however, we recover the main results of rather general theoretical studies on the formation of a collimated outflow from a magnetized and rotating astrophysical object. Nevertheless, for a meaningful comparison with the observations one needs to relax these assumptions, a task taken up in the next paper.

Acknowledgements. S.V. Bogovalov is grateful to the University of Crete for financial support of his visit during collaborative work on this problem and to K. Tsinganos for warm hospitality. BSV is also grateful to the director of the Astrophysics Institute of MEPhI Yu. Kotov for support of this work in Moscow. Work of BSV was partially supported also by RFBR grant N 96-02-17113. This research has been supported in part by a PENED grant from the General Secretariat for Research and Technology of Greece.

REFERENCES

Begelman, M., Li Z., 1994, ApJ, 426, 269.
Biretta, T., 1996, in *Solar and Astrophysical MHD Flows*, K. Tsinganos (ed.), Kluwer Academic Publishers, 357
Blandford, R.D., Payne, D.G., 1982, MNRAS, 199, 883 (BP82)
Bogovalov, S.V., 1992, Sov. Astron. Letts, 18(55), 337
Bogovalov, S.V., 1994, MNRAS, 270, 721
Bogovalov, S.V., 1995, Astron. Letts, 21, 4
Bogovalov, S.V., 1996, MNRAS, 280, 39
Bogovalov, S.V., 1997, A&A, 327, 662
Burderi, L., King, A.R., 1995, MNRAS, 276, 1141
Burrows, C.J., et al, 1995, ApJ, 452, 680
Cao, X., 1997, MNRAS, 291, 145
Chiueh, T., Li, Z.-Y, Begelman, M.C., 1991, ApJ, 377, 462
Crane, P., Vernet, J., 1997, ApJ, 486, L91
Contopoulos, J., Lovelace, R.V.E., 1994, ApJ., 429, 139
Eichller, D., 1993, ApJ, 419, 111
Ferrari, A., Massaglia, S., Bodo, G., Rossi, P., 1996, in *Solar and Astrophysical MHD Flows*, K. Tsinganos (ed.), Kluwer Academic Publishers, 607
Ferreira, J., 1997, A&A, 319, 340
Ferreira, J., & Pelletier, G., 1995, A&A, 295, 807
Goodson, A.P., Winglee, R.M., Bohm, K.H., 1997, ApJ, 489, 199
Heyvaerts, J., Norman, C.A., 1989, ApJ, 347, 1055
Jones, D.L., Wehrle, A.E., 1994, ApJ, 427, 221
Kafatos, M., 1996, in *Solar and Astrophysical MHD Flows*, K. Tsinganos (ed.), Kluwer Academic Publishers, 585
Kahabka, P., Trumper, J., 1996, in *Compact Stars in Binaries*, E.P.J. Van den Heuvel & J. van Paradijs (eds.), (Dordrecht: Kluwer), p. 425
Konigl, A., 1989, ApJ, 342, 208
Li, Z.-Y, Chiueh, T., Begelman, M.C., 1992, ApJ, 394, 459
Li, Z.-Y, 1995, ApJ, 444, 848
Li, Z.-Y, 1996, ApJ, 465, 855
Livio, M., 1997, in *Accretion Phenomena and Related Outflows*, D.T. Wickramasinghe, L. Ferrario, & G.V. Bicknel (eds.), ASP: San Francisco, (in press).
Livio, M., 1997, in *13^{th} North American Workshop on Cataclysmic Variables*, 14-19 June 1997, Jackson Hole, WI, USA
Meier, D.L., Edgington, S., Godon, P., Payne, D.G., Lind, K.R., 1997, Nature, 388, 350
Low, B.C., Tsinganos, K. 1986, ApJ, 302, 163
Michel, F.C., 1969, ApJ, 158, 727
Mirabel, I.F., Rodriguez, L.F., 1996, in *Solar and Astrophysical MHD Flows*, K. Tsinganos (ed.), Kluwer Academic Publishers, 683
Nerney, S.F., Swess, J., 1975, ApJ, 196, 837
Suess, J., 1972, J. Geophys. Res., 77, 567
Ostriker, E.C., 1997, ApJ, 486, 306
Ouyed, R., & Pudritz, R.E., 1997a, ApJ, 482, 712
Ouyed, R., & Pudritz, R.E., 1997b, ApJ, 484, 794
Parker, E.N. 1963, in: Interplanetary Dynamical Processes, Interscience Publishers, New York
Pelletier, G., Pudritz, R.E., 1992, ApJ, 394, 117
Ray, T.P., 1996, in *Solar and Astrophysical MHD Flows*, K. Tsinganos (ed.), Kluwer Academic Publishers, 539
Ray, T.P., Mundt, R., Dyson, J.E., Falle, S.A.E., Raga, A., ApJ, 468, L103.
Li, Z.-Y, 1996, ApJ, 465, 855
Romanova, M.M., Ustyugova, G.V., Koldova, A.V., Chechetkin, V.M., Lovelace, R.V.E., 1997, ApJ, 482, 708
Sakurai, T. 1985, A&A, 152, 121
Sakurai, T. 1987, PASJ, 39, 821
Sakurai, T. 1990, Computer Phys. Rep., 12(4), 247
Sauty, C., Tsinganos, K., 1994, A&A, 287, 893 (ST94)
Shahbaz, T., Livio, M., Southwell, K.A., Charles, P.A., 1997, ApJ, 484, L59
Shakura, N.I., Sunyaev, R.A., 1973, A&A, 24, 337
Shu, F., Najita, J., Ostriker, E., Wilkin, F., Ruden, S., Lizano, S., 1994, ApJ, 429, 781
Tomimatsu, A., 1994, PASJ, 46, 123
Tsinganos, K.C., 1982, ApJ, 252, 775
Vlahakis, N., Tsinganos, K., 1997, MNRAS, 292, 591
Vlahakis, N., Tsinganos, K., 1998, MNRAS, 298, 777
Washimi, H., Shibata S., 1993, MNRAS, 262, 936
Washimi, 1990, Geophys. Res. Letts., 17(1), 33
Weber, E.J., Davis, L.J. 1967, ApJ, 148, 217